Reinterpretation of catenary vaulted spaces: Construction of a prototype and structural evaluation through Multibody Rope Approach

Reinterpretarion of catenary vaulted spaces: Construction of a prototype and structural evaluation through Multibody Rope Approach

Giuseppe Fallacara[1], Ilaria Cavaliere[1], Jonathan Melchiorre[2], Giuseppe Carlo Marano[2], Amedeo Manuello[2]

[1] Department of Architecture, Construction and Design, Politecnico di Bari, Italy
[2] Department of Structural, Geotechnical and Building Engineering, Politecnico di Torino
*ilaria.cavaliere@poliba.it

Abstract. The paper aims to describe an innovative way to build catenary-shaped structures by fixing the geometry of a hanging chain through welding. This works according to the principle of the inverted catenary arch. The obtained catenary frames can be used to create architectural pavilions.

A preliminary case study inspired by the Chapel of the Holy Shroud, designed by the Italian Architect Guarino Guarini is presented. The Chapel is built with a series of entwined superimposed arches In the second part, the study for the realization of a prototype composed of a "winged structure" that has been built and exposed in Turin in June 2023 is reported.

Both the configurations are described and an evaluation of their behavior is presented. Their shape has been compared to a corresponding funicular form.

The digital representation of these structures is made using the multi-body rope approach (MRA).

Different MRA enhancing strategies are explained and discussed.

Keywords: Catenary Arch, Formfinding, Multi-body Rope Approach, Funicularity.

Introduction

This paper aims to describe a multidisciplinary research that merges architectural design with structural analysis to create structures with a geometry based on the catenary curve. A new construction process to realize catenary arches through the use of metallic chains will be presented and the case study of a pavilion built using this method will be described.

A catenary curve is defined as the configuration of a hanging string left free to hang under its own weight after its ends have been fixed to supports [1].

A hanging string is subject only to tensile stresses and if its shape is "frozen" and reversed, it will be subject to sheer compression stresses.

Robert Hooke was the first to define this principle in 1675. It is known as the "reversed catenary" principle [2]. The reversed catenary is the most suited frame for structures that work mainly in compression (vaults and arches) because it implies the absence of shear stresses.

Arches are stable only if the line of force, that is a catenary curve, lies within their own thickness: in the past, this principle was often used to evaluate the stability of masonry arched structures [3].

Antoni Gaudí is famous for the use of catenary geometries in his architecture. He was also one of the first architects to use models made of hanging ropes to empirically design optimized structures [4] (see Fig.1).

Insert Figure 1 here

The attic of Gaudí's Casa Milà, for example, is covered by a vault composed of a series of catenary arches (see Fig. 2); the corridor of the School of Teresianas is characterized by an array of parabolic arches, that behave similarly to catenaries [5].

Insert Figure 2 here

This geometry is used also in modern masonry structures, especially because computational design tools have eased the process of designing catenary curves thanks to digital algorithms and simulators.

In 2017 Giuseppe Fallacara and Maurizio Barberio designed and realized Flux, a temporary stone pavilion whose geometry derived from a network of catenary edges to guarantee the prevalence of compressive stresses [6].

The Saint Dizier's market, designed by Studiolada in 2023 is another interesting example of modern masonry architecture. It consists of a parallelepiped volume with walls made of stone. Each side is characterised by various openings shaped as catenary arches of different proportions [7].

The use of geometries based on catenary can be a strategy for architectures made of other materials that behave well under compression stresses, for example, raw earth.

In 2016 the studio Wallmakers designed the St. George Orthodox Church conceiving it as a vaulted structure made of raw earth bricks and characterized by catenary geometries [8].

Even if catenary curves are now easy to represent thanks to CAD tools, they are difficult to realize. They often require profiles created using a Computer Numerical Control (CNC) machine or are created through approximation. Both these conditions can be avoided using a "frozen" hanging chain.

Metal arches can be employed to build architectural installations (meant as temporary structures for exhibitions) or also to realize centring systems for vaulted spaces based on the catenary geometry. A centring system is a system of supports used to correctly place the ashlars of a vaulted system. Centrings are usually made of wood and their profile is shaped to follow the exact curvature of the vault. In the case of a catenary profile, a welded chain would help obtain the correct frame more easily than a custom wooden centring and it would produce less waste material.

Recent developments in computing technology have created new opportunities for structural engineering research, especially when it comes to finding the best possible structural shapes [9, 10]. The development of digital instruments, including computer simulations and calculators, has made it much easier to experiment with different form-finding techniques [11–14].

The Multibody Rope Approach (MRA) [15–17] is one of the many form-finding techniques that has gained popularity because it defines the funicular configuration of structures representing them as a net of linked nodes connected by slack ropes. This method models the structure as a system of falling bodies interconnected by slack ropes and looks for the funicular shape that fits the given loading circumstances. MRA finds the ideal configuration—where the tension in the ropes is in balance—by taking into account the equilibrium of forces within the system, producing a stable and structurally sound structure. Typically, the technique is used to define the ideal geometry for free-form gridshell structures [18–20].

In this work, the best structural form for an initial case study design modelled after Guarino Guarini's Chapel of the Holy Shroud is ascertained using the Multibody Rope Approach (MRA) [21]. The work focuses on the application of form-finding methods to distinguish between two different structural types: a funicular form under specified loading circumstances and a structural type consisting of catenary chains.

The next stage is to put these two structural configurations into a static self-weight loading study after they have been identified [22]. The stress distribution inside the structures can be assessed thanks to this research, which also makes it simpler to compare the more easily constructed catenary-based construction with the optimized funicular structure.

The study attempts to shed light on the trade-off between constructability and structural performance by measuring the stress distances between the two structural kinds. By emphasizing the variations in stress distribution and probable structural ramifications of selecting one form over the other, this study assists in guiding the decision-making process. In the end, the paper advances knowledge on how form-finding methods may support the process of design optimization by considering both structural effectiveness and practical practicality.

1 The catenary frame realization process

The proposed method, conceived by Giuseppe Fallacara, has been thought to realize catenary arches by welding the rings of a hanging chain and thus fixing its shape.

Before the real-scale experiment, some tests were conducted on small portions of the chain to verify the effectiveness of the technique.
Each end of the string was fixed to a horizontal bar and then the chain was left free to hang under its own weight, assuming the shape of a catenary curve. After that, all the rings were reciprocally welded in order to freeze the geometry (see Fig. 3).

Insert Figure 3 here

After some successful results, that showed that it was possible to weld a hanging chain maintaining the correct catenary shape, a real-scale experiment was conducted. A galvanized iron chain was used, with a rod of 20 mm and rings 7 cm wide and 10,2 cm high.
A portal-shaped structure made of metallic bars was previously built to hold the hanging chain, paying attention to the perfect horizontality of the architrave. This was fundamental because we wanted the catenary to be perfectly symmetrical.
After the chain was placed, the rings were welded (see Fig. 4). The final output of the experiment was an arch 2,75 m tall and 3,10 m wide (see Fig. 5).
It is important to underline that the welding process could be carried on without any deformation of the geometry thanks to the mass of the chain, which is 6,3 kg/m. The chain was chosen to take into account its mass, so that its high weight could prevent relevant movements in this phase and could guarantee a good result.

Insert Figure 4 here

Insert Figure 5 here

2 The assembly of the catenary arches

In the following Section, the first hypothesis for a pavilion made of metallic catenary arches will be described, and evaluations linked to the output of the structural analysis will be done.

2.1 A configuration inspired by Guarino Guarini

The first possible structure has been thought of as a tribute to the Italian architect Guarino Guarini.

Guarino Guarini's baroque architectures are famous for the sense of lightness and transparency because they are often designed through the intersection of arches [23]. Some examples are the dome of San Lorenzo and the Chapel of the Holy Shroud in Turin.

This last work has been the main inspiration for the first design proposal, which reinterprets the principle of the so-called "basket dome", which is a dome built through intertwined arches instead of a closed surface. Guarini's chapel is characterized by a series of staggered superimposed elliptical arches; there are different interpretations of their function, as some scholars consider them as purely decorative while others attribute them to a structural role [23].

The proposed structure is composed of three circular levels (see Fig. 6), each one composed of six catenary frames. The arches of the ground level (A_1A_3, A_2A_4) intersect each other (points B_1, B_2, B_3) the next level is made of other intersecting arches smaller than the previous ones, that are rotated so that the bases of the arches are placed in correspondence with the intersection points of the previous level (B_1B_3). The same goes for the third level, which is composed of the smallest frames (C_1C_3, C_2C_4).

In the following section, the real structural behaviour of the model will be discussed. In this case, even if the global structure is mainly subject to compression, shear stresses are not completely absent.

Insert Figure 6 here

2.2 Form-finding through the multi-body rope approach

2.2.1 Description of the method.

The Multibody Rope Approach (MRA), developed by [15], is a unique form-finding method designed to shape gridshell structures, accommodating highly free-form

geometries and diverse forming loads. Specifically tailored for gridshell structures employing standardized building components and embracing free-form designs, MRA leverages D'Alembert's principle to iteratively establish the ultimate equilibrium configuration for individual nodes within a dynamic model of falling bodies across both spatial and temporal domains. The proposed method involves identifying the funicular structural configuration using a system of nodal masses interconnected by slack ropes [24]. Initially, the masses are unrestrained by the slack ropes, allowing them to move freely. As the masses fall, the slack in the ropes gradually decreases until they become taut, restraining the movement of the masses. The dynamics of these falling masses are resolved iteratively until they reach a static equilibrium configuration, where the ropes are taut. This resulting hanging network configuration represents the funicular configuration of the system under the applied load. This method is devised for identifying the funicular structural configuration. The MRA method uses the nodal equations to define the equilibrium of a system of discrete particles. Specifically, the equilibrium condition of such a system represents the inverted configuration of a funicular structure with respect to the applied loads. By inverting the geometry obtained from the equilibrium solution of the system, it is then possible to obtain the funicular configuration which results to be the one optimized to support the applied loads.

The system of forces operating on individual nodes in MRA differs from that in the dynamic relaxation (DR) and spring-particle (SP) approaches. In particular, the method iteratively solves the physics of the system of nodal masses accelerating downward until their distance becomes such that they exceed the maximum length of the ropes. At this point, the ropes exert a pullback force on the masses that acts as a constraint on the nodes to which they are connected. To avoid numerical issues associated with infinitely large pullback forces, the method models these forces as nonlinear elastic forces. The elastic coefficient, denoted as *k*, is selected to ensure the ropes behave as effectively inextensible, maintaining numerical stability throughout the simulation.

It is important to note that no force is exerted when the distance between the ends is less than the predefined length of the rope (l_{rope}). The forces F applied to the end nodes may be represented as follows by specifying l as the distance between the rope two ends and k as the rope axial stiffness:

$$\begin{cases} F_{rope} = 0 \\ F_{rope} = k\left(l - l_{rope}\right) \end{cases} \quad if \quad \begin{matrix} l < l_{rope} \\ l \geq l_{rope} \end{matrix} \tag{1}$$

Where the rope length l_{ji} the distance between nodes i and j may be computed as:

$$l_{ji} = \sqrt{\left(x_j - x_i\right)^2 + \left(y_j - y_i\right)^2 + \left(z_j - z_i\right)^2} \tag{2}$$

In general, the MRA technique seeks to minimize axial deformations by assuming exceptionally high stiffness levels. Finding a geometric structure that guarantees the equilibrium of nodes exposed to external pressures and those emanating from ropes attached to them is the aim of MRA. Let us imagine a generic node (i) in the structural network of nodes and ropes, with mass m_i. Ropes connect the node i to a number n_i of additional nodes. If node i is subject to an external load p_i, the equilibrium equation may be expressed as follows:

$$\vec{R}_i = \vec{p}_i + \sum_{j=1}^{n_i} \vec{F}_{rope,ji} + \vec{F}_i^I + \vec{F}_i^{II} = 0 \tag{3}$$

The applied load $\vec{p}_i$, the forces transmitted by the ropes attached to the node ($\vec{F}_{rope,ji}$), the inertial force $\vec{F}_i^{II}$, and the damping force $\vec{F}_i^I$. are all combined to form the net force acting on node i in this equation, which is represented by the vector $\vec{R}_i$. Equation (4), which is the product of the node mass m_i and the magnitude of the acceleration vector a_i, may be used to compute the magnitude of the inertial force $\vec{F}_i^{II}$. The inertial force direction is opposite to that of the node acceleration.

$$\vec{F}_i^{II} = -m_i \cdot \vec{a}_i \tag{4}$$

The product of the velocity vector $\vec{v}_i$ with direction opposed to the velocity and a constant damping coefficient c_i yields the damping force $\vec{F}_i^I$. Equation (5) expresses this connection.

$$\vec{F}_i^I = -c_i \cdot \vec{v}_i \tag{5}$$

By expressing the generic node i as location as $\vec{u}_i = (x_i, y_i, z_i)$, the position in time may be derived to determine the acceleration and velocity, as shown in the relations (6).

$$\begin{aligned} \overrightarrow{v_\iota} &= \dot{\vec{u}}_\iota = (\dot{x}_\iota, \dot{y}_\iota, \dot{z}_\iota) \\ \vec{a}_i &= \ddot{\vec{u}}_\iota = (\ddot{x}_\iota, \ddot{y}_\iota, \ddot{z}_\iota) \end{aligned} \qquad (6)$$

Consequently, we may rewrite equation (3) as in (7).

$$\vec{R}_i = \vec{p}_i + \sum_{j=1}^{n_i} \{k \cdot \vec{F}_{rope,ji}\} - c_i \cdot \vec{v}_i - m_i \cdot \vec{a}_i = 0 \qquad (7)$$

Ultimately, the system of equation (8) may be obtained by projecting the equilibrium equation (7) into the three dimensions of space.

$$\begin{cases} \vec{p}_{ix} + \sum_{j=1}^{n_i} \left\{ \frac{(x_j - x_i)}{l_{ji}} \cdot \vec{F}_{rope,ji} \right\} - c_i \cdot \dot{x}_\iota - m_i \cdot \ddot{x}_\iota = 0 \\ \vec{p}_{iy} + \sum_{j=1}^{n_i} \left\{ \frac{(y_j - y_i)}{l_{ji}} \cdot \vec{F}_{rope,ji} \right\} - c_i \cdot \dot{y}_\iota - m_i \cdot \ddot{y}_\iota = 0 \\ \vec{p}_{iz} + \sum_{j=1}^{n_i} \left\{ \frac{(z_j - z_i)}{l_{ji}} \cdot \vec{F}_{rope,ji} \right\} - c_i \cdot \dot{z}_\iota - m_i \cdot \ddot{z}_\iota = 0 \end{cases} \qquad (8)$$

One way to solve the system of equations is to take Δt as a time increment. It is assumed that each node i has zero initial velocities and accelerations ($v_i(0) = 0$ and $a_i(0) = 0$), and that the nodes' locations at time t=0 are known. Each node location, velocity, and acceleration at time t may be used to calculate these values at the next instant, $t + \Delta t$. In order to do this, equation (9) illustrates how a coefficient C_3 may be defined as a function of the known node locations at time t^*.

$$C_3 = \vec{p}_i + \sum_{j=1}^{n_i} \{k \cdot \vec{F}_{rope,ji}\} \qquad (9)$$

The vector F_{rope}. is defined by the coefficient C_3, which is only dependent on the nodes' positions at time t^*. As a result, Equation (7) may be rewritten as demonstrated in (10).

$$\ddot{\vec{u}}_\iota + \frac{c}{m}\dot{\vec{u}}_\iota = C_3 \tag{10}$$

Furthermore, the system natural frequency ω_n and critical damping ζ may be expressed as follows in equations (11) and (12).

$$\omega_n = \sqrt{\frac{k}{m}} \tag{11}$$

$$\zeta = \frac{c}{2\omega_n m} \tag{12}$$

where m is the mass, c is the damping coefficient, and k is the stiffness of the system. When the system is not being affected by any outside forces, it vibrates at a frequency known as the natural frequency, or ω_n. The system is said to be critically damped when it returns to its equilibrium condition as soon as feasible without fluctuating; this is indicated by the damping coefficient value known as the critical damping, or ζ.

As a result, the following non-homogeneous second-order differential equation is found:

$$\ddot{\vec{u}}_\iota + 2\omega_n\zeta\dot{\vec{u}}_\iota = C_3 \tag{13}$$

By adding the specific solution to the related homogeneous differential equation, which is written as (14), the solution to equation (13) may be found.

$$\vec{u}(t) = C_1 e^{-2\omega_n\zeta} + C_2 + \frac{C_3}{2\omega_n\zeta}t \tag{14}$$

The system starting circumstances may be used to derive the coefficients C_1 and C_2. In this instance, they may be acquired by applying the nodes' locations and velocities at instant $t - \Delta t$, which is demonstrated in the following equations:

$$C_1 = -\frac{2\omega_n\zeta\dot{\vec{u}}_{(t-\Delta t)} - C_3}{(2\omega_n\zeta)^2} \tag{15}$$

$$C_2 = -\frac{(2\omega_n\zeta)^2\vec{u}_{(t-\Delta t)} + 2\omega_n\zeta\dot{\vec{u}}_{(t-\Delta t)} - C_3}{(2\omega_n\zeta)^2} \tag{16}$$

The locations, velocities, and accelerations of the system nodes at the preceding time instant determine the values of the coefficients C_1, C_2, and C_3 in the solution. Gradually, the locations of the nodes at successive instants may be computed, beginning with the starting condition when the nodes' location in three-dimensional space is known and their velocity and acceleration are zero. By calculating the difference between the nodes' locations at instants $t - \Delta t$, and dividing by the time increment Δt, one may derive the velocity vector ($\vec{\dot{u}}_t$).

$$\vec{\dot{u}}_t = \frac{\overrightarrow{u_t} - \overrightarrow{u_{t-\Delta t}}}{\Delta t} \tag{17}$$

Finally, by calculating the ratio of the incremental change in velocity between two time instants t - Δt and t, the acceleration ($\vec{\ddot{u}}_t$)˘may be found. To be more precise, this may be done by dividing the difference in velocity between the two by the time interval Δt.

$$\vec{\ddot{u}}_t = \frac{\overrightarrow{\dot{u}_t} - \overrightarrow{\dot{u}_{t-\Delta t}}}{\Delta t} \tag{18}$$

The suggested approach is made to determine a gridshell ultimate configuration from its starting mesh, which stands for the net beginning condition. Equations (14), (17), and (18) may be used in a sequential manner to find the new locations, velocities, and accelerations of nodes since their beginning positions are known and their initial velocities and accelerations are assumed to be zero. Until an equilibrium configuration representing the ideal structural geometry in relation to the applied force field $\vec{p}$ is achieved, this procedure is repeated.

The nodal masses m, the system stiffness k, the damping parameters c, the rope slack coefficient ρ, and the applied force field $\vec{p}$ all influence the calculated structural geometry. Equation (19). defines the slack coefficient ρ as the ratio of the starting distance between nodes to the goal length of the ropes.

$$\rho_{ij} = \frac{l_{rope}}{\overrightarrow{u_i}(0) - \overrightarrow{u_j}(0)} = \frac{l_{rope}}{\sqrt{(x_i - x_j)^2 + (y_i - y_j)^2 + (z_i - z_j)^2}} \tag{18}$$

Generating a structural geometry that is ideal for simplicity of construction and structural efficacy is the goal of using MRA. The number of beam components of the same length is used as a metric to assess the simplicity of construction. In reality, as the number of components to be constructed rises, so does the complexity of assembling a gridshell. Therefore, while considering a specific tolerance toll, it is essential to ascertain the number of pieces in the final configuration that have a length equal to the goal length l_{rope}.

2.2.2 Structural analysis of the preliminary case study

Guarino Guarini's Chapel of the Holy Shroud served as the model for the structural shape seen in Fig. 6, which was obtained by using the Multibody Rope Approach (MRA). Initially, the MRA was applied to individual chains to evaluate the method efficacy in creating catenary geometries. Through an analysis of these chains' behaviour, the requisite catenary designs were discovered. These catenaries were then layered to form the whole geometry of the building. In addition, to this method, the MRA was directly applied to the entire structure in order to do a comparison study. This made it possible to ascertain the structure funicular form when self-weight loading was applied. The MRA was able to precisely identify the ideal structure by taking the whole thing into consideration. In this scenario, the structural form differs from that comprised solely of catenary arches. This discrepancy arises from the overlapping of the arches, which introduces a non-uniform load condition. Specifically, the upper arches exert a concentrated force at the points of connection to the lower arches. As a result, the funicular configuration deviates from the configuration formed by individual catenary arches. The construction was analysed with the FEM SOFiSTiK program [22], based on the assumption that they consisted of a 3 cm-diameter solid steel cable. The study was carried out with the structure self-weight in mind. The computed load per linear meter was found to be 5.5 kg/m based on this assumption. Fig. 7 presents the analytical findings, including Von Mises stress and internal activities. The results clearly show that, in terms of construction, the funicular structure is the better option. This is because the funicular structure displays a bending moment of zero, which is consistent with what is expected for a form of that kind. As a result,

the funicular structure only experiences 15% of the stress experienced by the catenary-composed structure. In light of the 6.3 kg weight per linear meter of the actual chain utilized in the building of the structure, an adjustment factor of 1.15 must be applied to the internal action and stress values displayed in Fig. 7. The real internal activity and stress values that the structure experiences may be found by multiplying the numbers in Figure 3 by this factor. Furthermore, it is crucial to recognize that the catenary structure has benefits from a building perspective and fits in nicely with the method outlined in the previous Section. When compared to the funicular construction, this design turns out to be more practical and simpler to build. Furthermore, it is important to remember that, even with the funicular form structural efficiency, the stresses placed on both structures are still much below the structural steel yield strength. This suggests that neither shape exceeds the limit of their material strength and that they both demonstrate a sufficient degree of structural integrity to safely bear the applied stresses.

Insert Figure 7

The funicular shape offers a good balance between constructional simplicity and structural effectiveness in this situation. It offers practicality and convenience of building at the same time as providing a reasonable level of structural performance. This makes it an appealing and feasible solution for achieving the intended architectural design while taking the practical and technical aspects of building into account.

As the study revealed, the frame is no longer optimized to withstand sheer compression loads if the global structure is made up of a composition of intertwined catenary arches since a funicular geometry will be the most efficient structure.

2.3 The prototype of a winged pavilion

There are other configurations that can be obtained through the assembly of catenary arches besides the pavilion previously described.

The number of arches and levels can vary, producing different patterns.

Also, completely different geometries can be realized, not necessarily referring to domes but also to other kinds of vaults.

Fig. 8 shows another pavilion designed as a “winged” structure that has been realized on the occasion of the IWSS conference held in Turin in June 2023 (https://sites.google.com/view/iwss/iwss2023).
The prototype is composed of three identical catenary arches, each one 2.75 m tall and 3.10 m wide. One of the three frames was placed to lie in a vertical plane, while the other ones lay on oblique planes, creating overhangs of about 45°. Fig. 8 shows the main dimensional characteristics of the pavilion.

Insert Figure 8

The three arches are connected to each other through a network made of elastic ropes, that are placed to create two saddle-shaped profiles and help improve the stability of the structure by balancing it. Each saddle represents one of the “wings” of the pavilion. The chosen rope has a diameter of 7 mm.
The construction process required two phases: the assembly of the metallic structure and the creation of the network of ropes.
The construction of the metallic skeleton took place at Sider Zzinox in Corato (BA, Italy). After the three arches had been welded, the assembly consisted of the following steps. First of all an H-shaped base was created using three iron bars. The two lateral bars have a rectangular cross-section of 5 x 15 mm and they were provided with a couple of metallic pierced plates, which were welded on the center of one of the faces of the bar. They were used to fix these bars to the central one using bolts. Another couple of plates were welded on the center of the adjacent face, where the ends of the three arches converged so that they could be fixed using bolts as well (see Fig. 9). The central transversal bar has a rectangular cross-section of 5 x 20 mm and it is in charge of nullifying the pressure produced by the arches. After this the first arch was placed and its inclination was fixed through two oblique iron bars screwed at the base. Successively, the central arch was placed and fixed to the previous one using another oblique iron bar. Finally, the third arch was placed and fixed to the previous one and to the base with two iron bars.

Insert Figure 9

After the assembly, the structure was transferred to the Valentino Castle in Turin, where it was completed with a network of ropes.
Two different patterns were used for the wings, one denser than the other, as shown in Fig. 10.

Insert Figure 10

Insert Figure 11

3 Discussion and conclusions

The proposed configurations are only two of many more possible ones that can be realized using metallic frames.
However, the described method to realize catenary arches through welding can be useful also for applications linked to the construction industry. For instance, it can be used to build a system of centrings. They can have a simple structure – for example an array of metallic arches reciprocally connected by metallic bars – or also a more complex one – for example, the winged structure itself can become a centring for a complex vaulted space (see fig. 12).

Insert Figure 12

Creating centrings by fixing the form of hanging strings helps spare materials since wooden frames inevitably produce material waste. Moreover, the construction process of a wooden centring would be more complex and would require CNC machines, differently from the proposed construction process, that requires only a welding phase. Through this method catenary profiles can be easily produced directly from hanging chains, and this helps avoid both approximations and complex fabrication processes with CNC machines.

This flexible method could also be used to realize non-symmetrical arches through the variation of the reciprocal height of supports to which the hanging string is fixed.
Despite there are numerous pros, some cons must be highlighted.
First of all, the global structure must be simple to work under sheer compression: in fact, a catenary is a curve optimized only under the self-weight load. A composition of more catenaries does not correspond to an optimized structure because each arch is subject to other loads and not only to gravity In this condition shear stresses will be present.
Moreover, there is a consistent problem linked to transportation: welded chains cannot be disassembled, can be large and very heavy and transporting them from the production site to the construction site can be difficult. Therefore, this method would be more convenient only if applied on site.
From a structural standpoint, Section 2.2.2 demonstrates that utilizing the Multibody Rope Approach (MRA) for the form-finding of funicular structure results in more structurally efficient geometries. However, the stresses associated with the funicular shape are not significantly different from those obtained with the pure catenary shape. This indicates that the catenary geometry remains a viable solution that strikes a balance between structural efficiency and ease of construction.
While the catenary geometry may not represent the structural optimum, it offers advantages in terms of aesthetics and construction simplicity. The method proposed in this paper for defining the catenary structure directly on-site facilitates the structural shape definition compared to constructing a more complex funicular geometry. The catenary form balances structural performance with practical construction considerations, making it a suitable choice for many real-world applications where both factors need consideration.
These considerations also extend to the prototype of the winged pavilion. In this case, loads are applied to the chains through the ropes net, resulting in forces not lying on the catenary plane. From a structural perspective, this implies the occurrence of out-of-plane stresses. Nevertheless, the catenary form provides a satisfactory solution that aligns with the overall objectives of the project.
A promising direction for future research could involve a more thorough examination of utilizing welded chains in the establishment of centring systems for vaulted ceilings.

Moreover, exploring the integration of weights strategically hung at specific chain points could offer an innovative approach to constructing funicular shapes using the methodologies introduced in this study.

Acknowledgments

The prototype described in this paper has been designed by Giuseppe Fallacara, who also invented the construction process of catenary arches through the welding of chains. The fabrication process took place at Sider Zzinox, in Corato (Italy).
Ilaria Cavaliere contributed to the design phase of the prototype and took part to the assembly phase in Turin.
Jonathan Melchiorre, Amedeo Manuello and Giuseppe Carlo Marano worked on the 3D modelling using the multi-body rope approach and on the structural analyses.
All authors read and approved the final manuscript.

References

1. Gohnert M., Bradley R. (2020) Catenary Solutions for Arches and Vaults. Journal of Architectural Engineering 26(2).
2. Gohnert M., Bulovic I., Bradley R. (2018) A Low-cost Housing Solution: Earth Block Catenary Vaults, Structures 15:270-278.
3. Block P., DeJong M., Ochsendorf J. (2006) As Hangs the Flexible Line: Equilibrium of Masonry Arches, Nexus Network Journal 8:13-24.
4. Tomlow J. (2011) Gaudí's reluctant attitude towards the inverted catenary. Engineering History and Heritage 164(EH4).
5. Huerta S. (2011) Structural Design in the Work of Gaudí. Architectural Science Review 49(4):324-339.
6. Fallacara G., Barberio M. (2018) An Unfinished Manifesto for Stereotomy 2.0. nexus Network Journal 20:519-543.
7. Saint Dizier's Market / Studiolada. Archdaily https://www.archdaily.com/1007805/saint-diziers-market-studiolada, last aaccessed 2024/01/11
8. St George Orthodox Church / Wallmakers. Archdaily,

https://www.archdaily.com/959657/st-george-orthodox-church-wallmakers, last accessed 2023/05/06.

9. J. Melchiorre, A. Manuello, F. Marmo, S. Adriaenssens, G. Marano, Differential formulation and numerical solution for elastic arches with variable curvature and tapered cross-sections, European Journal of Mechanics-A/Solids 97 (2023) 104757.
10. Rosso, M. M., Melchiorre, J., Cucuzza, R., Manuello, A., & Marano, G. C. (2022). Estimation of distribution algorithm for constrained optimization in structural design. WCCM-APCOM 2022, 900.
11. H.-J. Schek, The force density method for form finding and computation of general networks, Computer methods in applied mechanics and engineering 3 (1) (1974) 115–134.
12. J. R. H. Otter, A. C. Cassell, R. E. Hobbs, POISSON, Dynamic relaxation, Proceedings of the Institution of Civil Engineers 35 (4) (1966) 633–656.
13. P. Block, J. Ochsendorf, Thrust network analysis: a new methodology for three-dimensional equilibrium, Journal of the International Association for shell and spatial structures 48 (3) (2007) 167–173.
14. A. Kilian, J. Ochsendorf, Particle-spring systems for structural form finding, Journal of the international association for shell and spatial structures 46 (2) (2005) 77–84.
15. A. Manuello, Multi-body rope approach for grid shells: form-finding and imperfection sensitivity, Engineering Structures 221 (2020) 111029.
16. A. M. Bertetto, F. Riberi, Form-finding of pierced vaults and digital fabrication of scaled prototype, Curved and Layered Structures 8 (1) (2021) 210–224.
17. A. Manuello, J. Melchiorre, L. Sardone, G. C. Marano, Multi-body rope approach for the form-finding of shape optimized grid shell structures, in: Proceedings of the 15th World Congress on Computational Mechanics, 2022.
18. Manuello Bertetto, A., Melchiorre, J., & Marano, G. C. (2023, June). Improved Multi-body Rope Approach for Free-Form Grid Shells. In Italian Workshop on Shell and Spatial Structures (pp. 231-240). Cham: Springer Nature Switzerland.
19. Melchiorre, J., Soutiropoulos, S., Manuello Bertetto, A., Marano, G. C., & Marmo, F. (2023, June). Grid-Shell Multi-step Structural Optimization with Improved Multi-body Rope Approach and Multi-objective Genetic Algorithm. In Italian Workshop on Shell and Spatial Structures (pp. 62-72). Cham: Springer Nature Switzerland.
20. Melchiorre, J., Bazzucchi, F., Manuello Bertetto, A., & Marano, G. C. (2023, June). Postbuckling Echoes of iMRA Introduced Variation in Gridshells Mechanical Behaviour. In Italian Workshop on Shell and Spatial Structures (pp. 379-389). Cham: Springer Nature Switzerland.

21. Cavaliere, I., Fallacara, G., Manuello Bertetto, A., Melchiorre, J., & Marano, G. C. (2023, June). Multy Body Rope Approach and Funicular Prototype for a New Constructive System for Catenary Arches. In Italian Workshop on Shell and Spatial Structures (pp. 259-268). Cham: Springer Nature Switzerland.
22. SOFiSTiK, Text Editor 2023, Flataustr. 14, 90411 Nuremberg, 2022. URL https://www.https://www.sofistik.com
23. Mazziotti A., Brandonisio G., Lucibello G De Luca A. (2017) Structural Analysis of the Basket Dome in the Chapel of the Holy Shroud by Guarino Guarini. International Journal of Architectural Heritage 11(3).
24. Bertetto, A. M., Melchiorre, J., & Marano, G. C. (2024). Improved multi-body rope approach for free-form gridshell structures using equal-length element strategy. Automation in Construction, 161, 105340.

Figures

Fig. 1. Gaudi's Hanging Weights Model, picture courtesy eeetthaannn available at: https://flic.kr/p/2g24Jcm (CC BY-NC 2.0).

Fig. 2. Casa Milà attic, picture courtesy of Keith Ewing available at: https://flic.kr/p/RG4vWn (CC BY-NC 2.0).

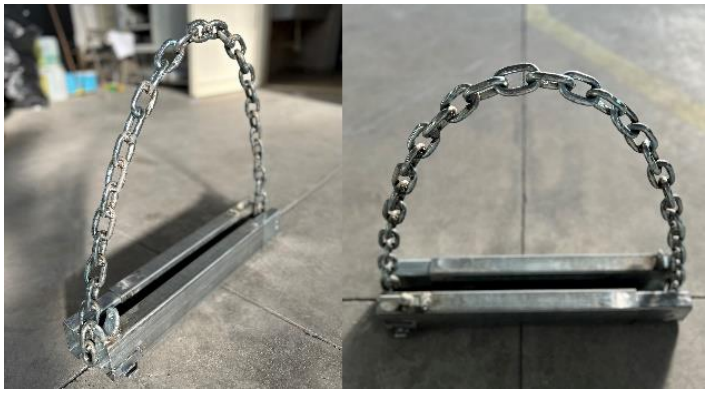

Fig. 3. A test conducted on a small chain.

Fig. 4. The welding phase of the real scale arch.

Fig. 5. The hanging chain that has been welded to obtain a catenary frame.

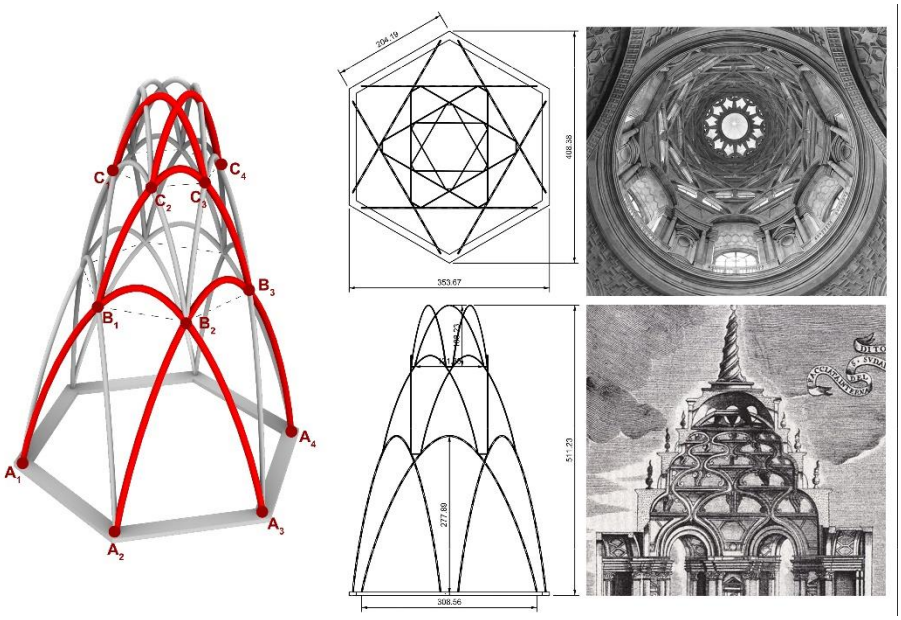

Fig. 6. A comparison between a scheme of the designed pavilion and the vault of the Chapel of the Holy Shroud.

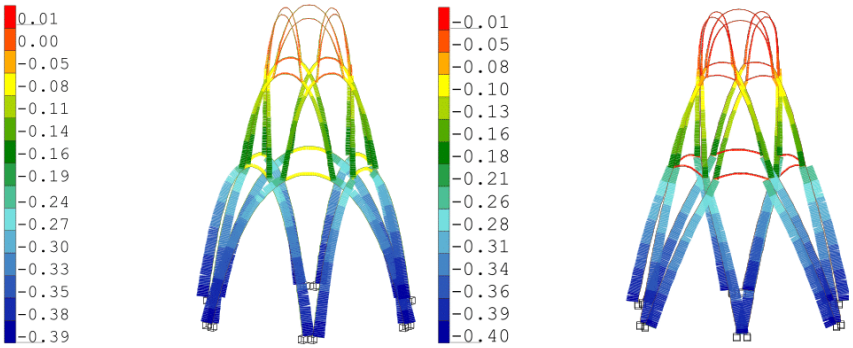

(a) Axial Force: $|N|_{max} = 0.39kN$ (b) Axial Force: $|N|_{max} = 0.40kN$

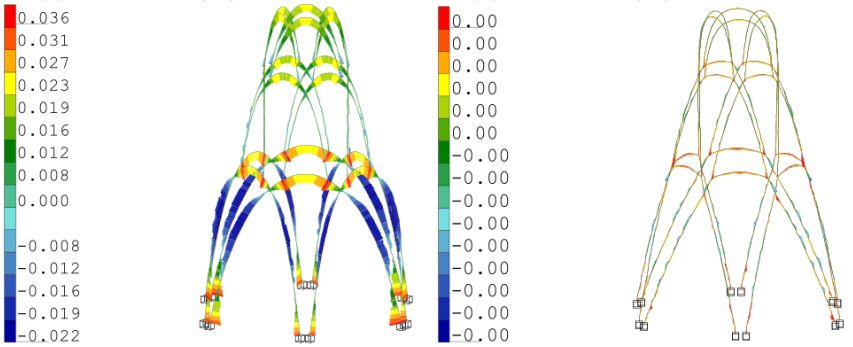

(c) Bending Moment: $|M|_{max} = 0.04kNm$ (d) Bending Moment: $|M|_{max} = 0kNm$

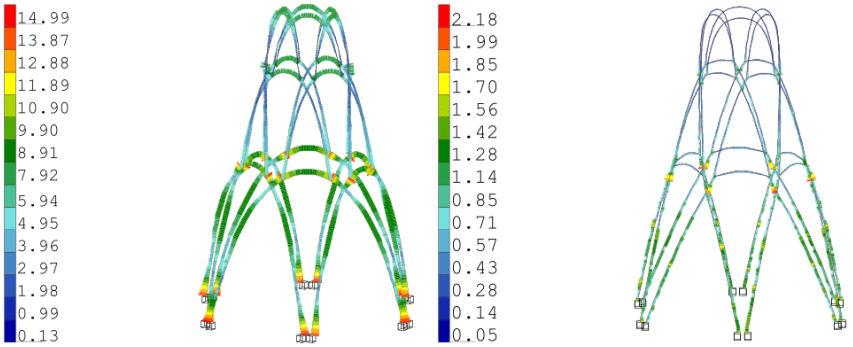

(e) V.M. Stress: $|\sigma^{VM}|_{max} = 14.99kPa$ (f) V.M. Stress: $|\sigma^{VM}|_{max} = 2.18kPa$

Fig. 7. Results of the static analysis on the two structural typologies inspired by the Chapel of the Holy Shroud by Guarini. Catenary shape on the left and funicular shape on the right.

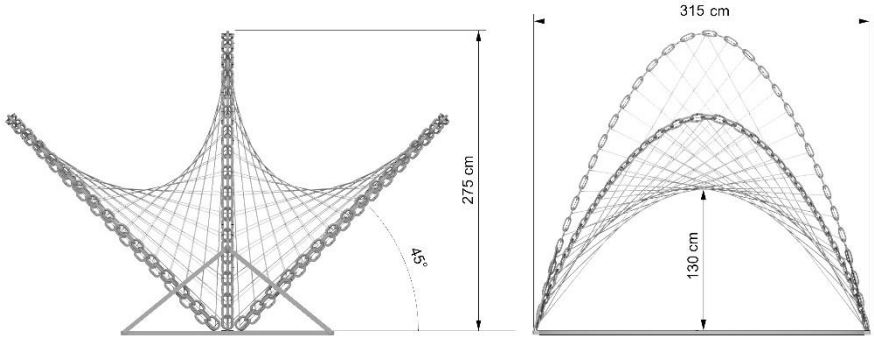

Fig. 8. A scheme of the designed structure with the main dimensions.

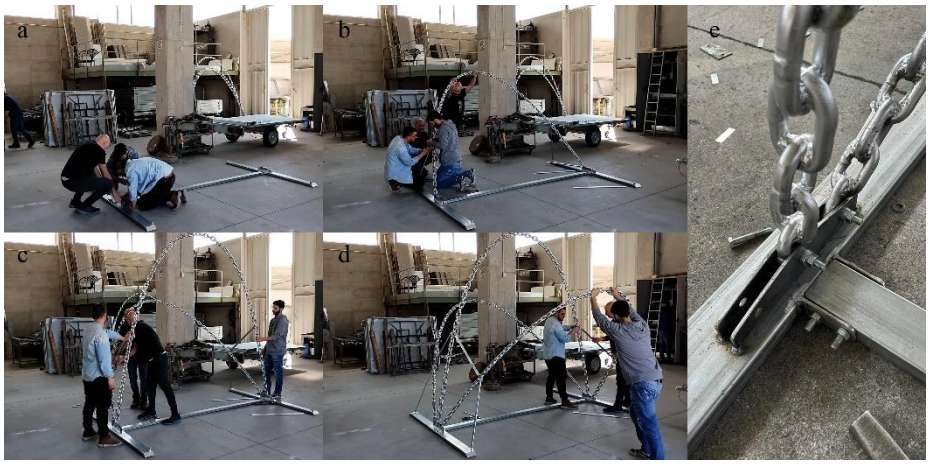

Fig. 9. The assembly phases of the metallic frame: a) assembly of the base; b) placement of the first arch; c) placement of the second arch; d) placement of the third arch; e) a detail of the assembly system.

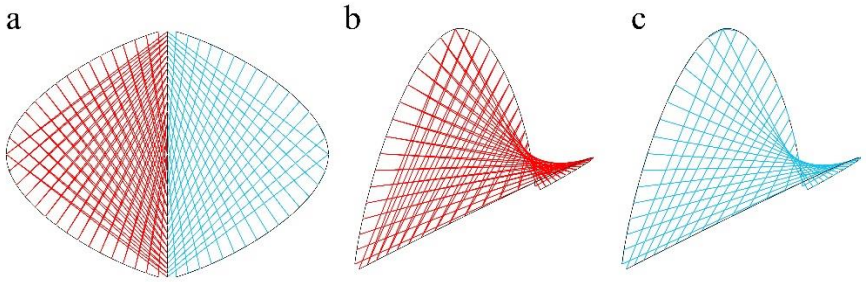

Fig. 10. A scheme of the two different networks: a) top view of the two pattern; b) denser network; c) thinner network.

Fig. 11. The final prototype in front of the Valentino Castle.

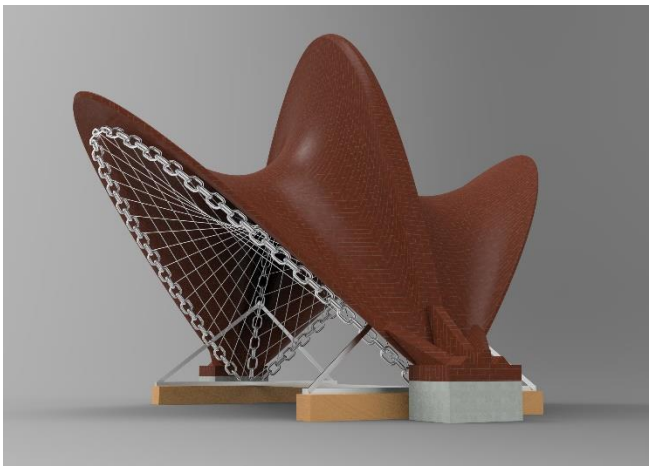

Fig. 12. A rendering showing how the winged pavilion can be used as a centring.